Volume 10, Issue 4, 2020, 5932 - 5937 ISSN 2069-5837
Biointerface Research in Applied Chemistry
www.BiointerfaceResearch.com
https://doi.org/10.33263/BRIAC104.932937
Original Research Article Open Access Journal
Received: 23.03.2020 / Revised: 19.04.2020 / Accepted: 20.04.2020 / Published on-line: 23.04.2020

Green synthesis of cerium oxide nanoparticles: characterization, parameters optimization and investigation of photocatalytic application

Asma Shojaee [1], Ali Mostafavi [1], Tayebeh Shamspur [1], Fariba Fathirad [2,*]
[1]Department of Chemistry, Faculty of Science, Shahid Bahonar University of Kerman, Iran
[2]Department of Nanotechnology, Graduate University of Advanced Technology, Kerman, Iran
*corresponding author e-mail address: ***f_fathirad@yahoo.com*** | Scopus ID 54782460500

ABSTRACT
In the present work, cerium oxide nanoparticles were synthesized using a very simple and green method. Egg white was used as a stabilizing agent in order to size and morphology control. The nanoparticles were obtained without any toxic and hazardous chemical agent at room temperature. The effective parameters on nanoparticles synthesis such as pH, amount of stabilizing agent and calcination temperature were optimized. The size and morphology of prepared nanoparticles were investigated and determined with XRD and FESEM. In optimum conditions, nanoparticles were synthesized with about 9 nm in size. The ability of the synthesized green oxide cerium nanoparticles was investigated as photocatalyst for the degradation of two dyes of malachite green and methyl orange. The experiments were carried out in visible light and ambient temperature and effective parameters on degradation process such as dye solution, pH, photocatalyst amount and process time were optimized. The obtained results show that the dye degradation happens as well in short time.
Keywords: *Green synthesis; Egg white as stabilizer; Photocatalyst; Methyl orange; Malachite green.*

1. INTRODUCTION
Cerium oxide, also known as ceric dioxide or ceria, is an oxide from the rare-earth metal of cerium. It is an important commercial product and an intermediate compound for the purification of the elements from the ores. Cerium oxide is a semiconductor material that has a large band gap (range of 3.0 and 3.2 eV) and a wavelength in UV area at around 370 nm [1-4]. The specific property of this compound is its reversible conversion to a non-stoichiometric oxide. This oxide has many applications in different fields of sciences due to unique properties. The main application of ceria is for polishing, especially chemical-mechanical planarization. It is used to decolorize glass by converting green-tinted ferrous impurities to colorless ferric oxides. In addition, CeO_2 has a range of other applications including sensor, O_2 storage, fuel cells, and cosmetics preparation. Along with all of these applications, cerium oxide and its nanostructured form are known materials as catalysts and photocatalyst in chemical processes [5-8]. Because of the great importance of nano-sized form of this oxide, several physical and chemical method were proposed for CeO_2 NPs synthesis with special shape and size. However, most of these used methods are time consumption and require complex conditions or create harmful and hazardous by-products [7-10]. In response to concerns about the potential risks associated with the use of hazardous materials in the synthesis of nanoparticles, green methods have been highly considered by applying a wide range of environment friendly and non-toxic solvents and precursors to the synthesis of various nanostructures. [11-17]. In this research, we have tried to use the principles of green chemistry to synthesize and optimize the cerium oxide nanoparticles. Recently, one of the natural materials used to synthesize nanoparticles is chicken egg white (CEW). Egg white is a natural and biological fluid that contains high levels of amino acids and proteins such as albumin and lysozyme. These amino acids structurally can play a stabilizing and controlling role in the synthesis of nanoparticles [18-20]. In similar studies, it is attempted to use commercially pure amino acids with high prices. But in this research has tried to use it directly from egg whites, which is affordable and inexpensive. We separated the protein from CEW using a commonly used freeze-drying method and investigated and optimized the effect of different parameters such as pH, amount of stabilizing agent and calcination temperature. Afterward, the nanoparticles were characterized by XRD and FESEM to obtain information about the effect of different parameters on mean crystallite size and morphology. Finally, the application of the best prepared CeO_2 NPs as photocatalyst for the elimination of two dyes of malachite green (MG) and methyl orange (MO) was studied.

2. MATERIALS AND METHODS
2.1. Materials and apparatus.
$Ce_2(SO_4)_4.4H_2O$ and NaOH were purchased from Merck. The crystallographic results and morphology were obtained using X-ray diffractometer (Rigaku D-max C III) and field emission-scanning electron microscope (CARL ZEISS-AURIGA, Germany). For recording the UV-Vis spectra a PerkinElmer UV-Vis spectrophotometer was used.

2.2. Synthesis of cerium oxide nanoparticles.
In order to prepare chicken egg withe (CEW) as a stabilizer for synthesizing CeO_2 nanoparticles, freeze-drying method was carried and the obtained powder was used without any purification. 0.5 mL of 0.1 M $Ce_2(SO_4)_4.4H_2O$ was added to a 10 mL aqueous solution containing 25 mg mL^{-1} CEW and solution was stirred vigorously. Then the pH was adjusted to 10 with NaOH solution (1 M). The solution was placed in oven at 37°C for 6 h. The obtained

sediment was separated with centrifugation at 4000 rpm, washed several time and dried in the oven at 60 °C. The nanoparticles were then calcined at 500 °C for 2 h and characterized using XRD and FESEM.

2.3. Photocatalytic activity of CeO_2

In order to investigate of photocatalytic activity of CeO_2 nanoparticles for MG and MO removal, 100 mL solution containing 50 ppm from each dye, separately was made using deionized water. 0.02 g and 0.005 g cerium oxide nanoparticles as photocatalyst were dispersed in MG and MO dye solutions, respectively by sonication and was placed under visible light for a specified time**.** The dye concentration was calculated by absorbance value measurement with a UV-Vis spectrophotometer.

3. RESULTS

3.1. Characterization of nanoparticles.

Several experiments were carried out to optimize the synthesis of CeO_2 NPs with the best size, morphology and subsequently photocatalytic performance. According to Table 1, different parameters such as the amount of $Ce(SO_4)_2$ (g) (A), egg white amount (B), calcination temperature (C) and pH (D) was investigated and optimized.

3.1.1. X-ray Powder Diffraction (XRD).

In order to investigate the calcination temperature effect on the green synthesis of nanoparticles, four samples were prepared according to the method described in section 2.2 at four calcination temperature: ambient temperature and in the furnace at temperatures of 100, 300 and 500°C. The obtained nanoparticles were called S1, S2, S3 and S4, respectively (Table 1). XRD patterns of synthesized CeO_2 nanoparticles are shown in Fig. 1. As shown, at calcination temperatures of 0 to 400 ° C, the temperature was not sufficient for the crystalline phase and pure oxide synthesis. With increasing calcination temperature up to 500 °C (Fig. 1S4), characteristic peaks related to the ceramic oxide crystalline phase appeared at 2θ of 10 to 80 degrees. The whole Bragg peaks are related to the face centered cubic (FCC) phase of cerium oxide (JCPDS No. 34-0394).

Table 1. Different conditions for CeO_2 NPs synthesis.

Sample	A (g)	B (g)	C (°C)	D
S1	0.02	2.5	25	6.0
S2	0.02	2.5	100	6.0
S3	0.02	2.5	300	6.0
S4	0.02	2.5	500	6.0
S5	0.02	0	500	2.0
S6	0.02	5.0	500	7.5
S7	0.02	2.5	500	3.0
S8	0.02	2.5	500	7.0
S9	0.02	2.5	500	10.0

To evaluate the effect of egg white amount as a stabilizing agent on the morphology and size of cerium oxide nanoparticles, 0, 2.5 and 0.5 g egg white were added to 100 mL distilled water and CEW solutions were prepared. Then, all steps were performed in accordance with section 2.2. The resulting samples called S5, S4 and S6, respectively. As shown in Fig. 1 (S5), there is a lot of impurities and noise in this pattern; nevertheless, oxide nanoparticles are synthesized. In Fig. 1(S6), noise is less than Fig. 1(S5), but the number of additional peaks and impurities has increased. The highest purity the smallest crystalline size, resulting in 2.5 g of egg white (Fig. 1 S4). Therefore, this amount was selected as optimum for the nanoparticles synthesis.

In order to investigate the effect of pH, three solutions with pH 3, 7 and 10 were prepared and then, according to section 2.2 cerium oxide nanoparticles were synthesized. The obtained samples called S7, S8 and S9. Because the alkaline medium is necessary to synthesize cerium oxide, no sediment was formed at pH= 3. At neutral pH, the amount of sediment yield was insignificant. According to table. 1, the best pH for NPs synthesis was selected 10.

Also, the average crystallite sizes for all samples were calculated using Scherrer's formula and shown in Table 2.

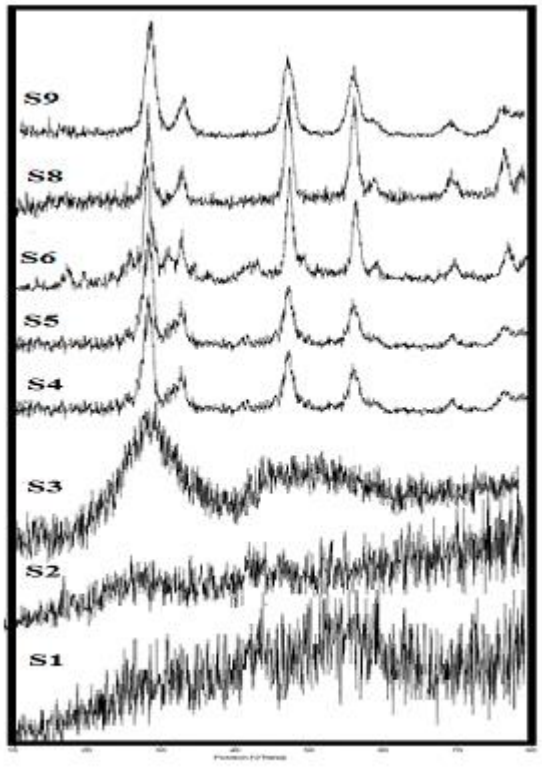

Figure 1. XRD patterns of as synthesized CeO_2 NPs.

Table 2. Average crystallite size of synthesized CeO_2 NPs

Sample	Average crystallite sizes (nm)
S1	-
S2	-
S3	-
S4	11.7
S5	53
S6	14.25
S7	-
S8	10.78
S9	8.91

3.1.2. Field emission scanning electron microscopy (FESEM).

Due to the main goal of this work is the green synthesis of cerium oxide nanopowders using egg white, the effect of egg white content on the synthesis process was investigated with FESEM images. As shown in Fig. 2, when the nanoparticles were synthesized in absent of egg whites (S5), the nanoparticles have been shaped like large agglomerates; their sizes have increased and, as a result, have not uniform morphology and the nanoparticle size is more than 100 nm. Figure 2(S9) shows FESEM images of synthesized nanoparticles in the presence of 2.5 g egg white. In this

image, the effect of egg white is well established, and all of them have uniform morphology and spherical shape. The average particle size is 23 nm. In Figure 2(S6), when the amount of egg white was 0.5 g, the nanoparticles size was thickened and non-uniform morphology was observed.

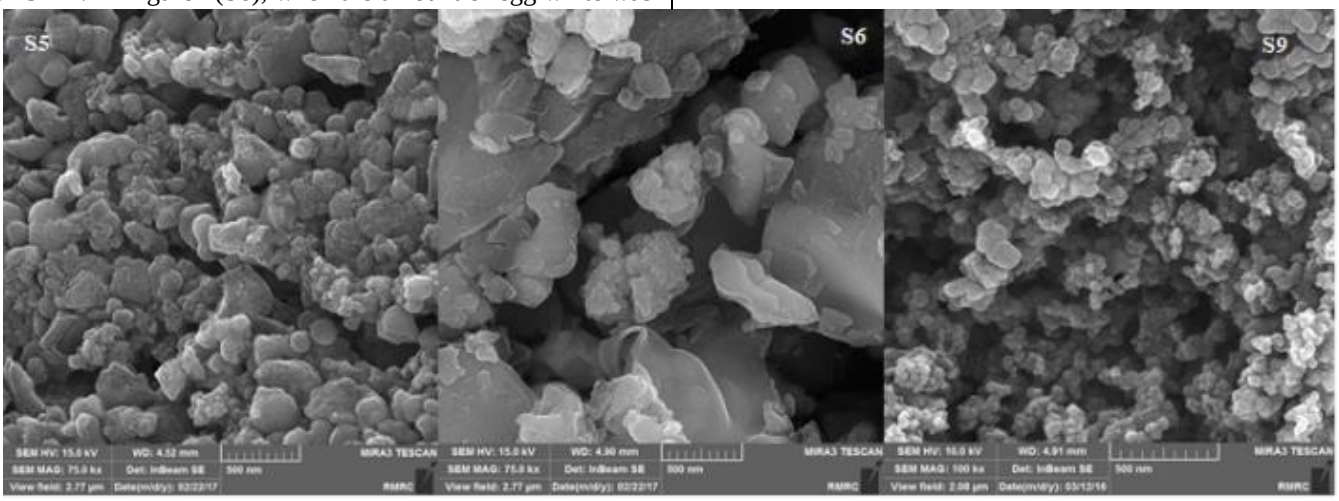

Figure 2. FESEM images of as synthesized CeO_2 NPs.

According to the results, the optimal condition for the green synthesis of cerium oxide nanoparticles was selected as sample S9. In the following, the ability of these nanoparticles as semiconductor photocatalyst for the degradation of two pollutant dyes was investigated.

3.2. Investigation of photocatalytic activity of CeO_2 nanoparticles for degradation of MG and MO.

The photocatalytic activity of prepared semiconductor nanoparticles as photocatalyst was investigated for two dyes of MG and MO. Fig. 3. shows UV-Vis spectra of photocatalyst for removal of MG (A) and MO (B) under visible light. The spectrum (a) shows a blank solution without photocatalyst and the spectrum (b) shows the photocatalytic performance of CeO_2 NPs in the presence of dyes.

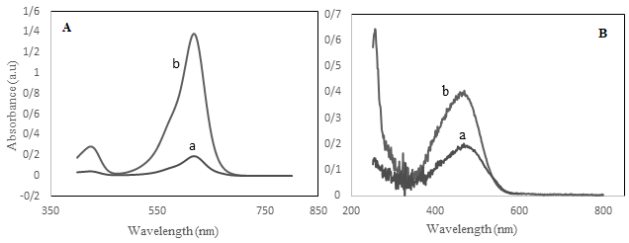

Fig. 3 Photocatalytic activity of CeO_2 nanoparticles in the removal of (A) MG and (B) MO dyes

3.2.1. Effect of pH

The influence of pH on the photocatalytic activity of CeO_2 was studied. As shown in Fig. 4(A), with changing pH from 6 to 9, the speed of MG dye removal was increased from 18% to 95% and after pH=9, the MG structure destroyed. Therefore, pH=9 was selected for the next experiments. As shown in Fig. 4(B), the MO removals increase in pH range of 3.0 to 4.0 and then decreases at higher values. Therefore, pH=4 was selected for the next experiments.

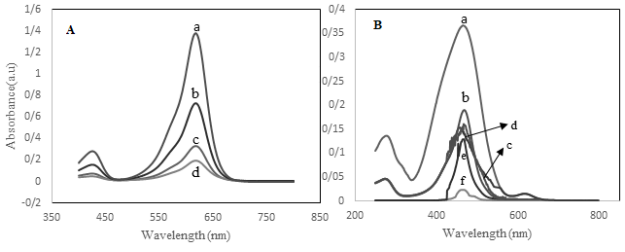

Figure 4. Effect of pH on photocatalytic activity and removal efficiency of: (A) MG and (B) MO dyes.

3.2.2. Effect of Photocatalyst Amount

For the investigation of photocatalyst amount effect on removal efficiency, the photocatalyst amount was varied from 0.005 to 0.04 g for MG and 0.003 to 0.04 g for MO and experiments were followed. As shown in Fig. 5, the increasing amounts would make the reaction faster due to the increase in the active sites number. Further increase in photocatalyst amount above 0.02 g for MG and 0.005 g for MO reduced the removal efficiency, which could be due to the hindrance to the pathway of light to reach the dye molecules. Therefore, 0.02 and 0.005 g were selected as optimum amounts.

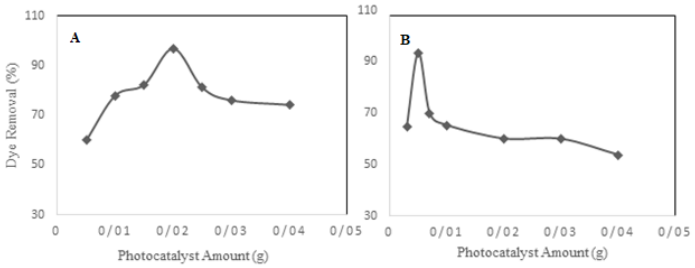

Figure 5. Effect of photocatalyst amount on removal efficiency of (A) MG and (B) MO dyes.

3.2.3. Effect of reaction time.

To evaluate the effect of the irradiation time on the removal efficiency of MG and MO, the solutions were exposed to visible light at 5 to 55 min. In the beginning, due to the presence of high amounts of dyes in the solution, the rate is high and removal efficiency is increased but is fixed after 45 minutes (Fig. 6). Therefore, the reaction time of 45 min was selected.

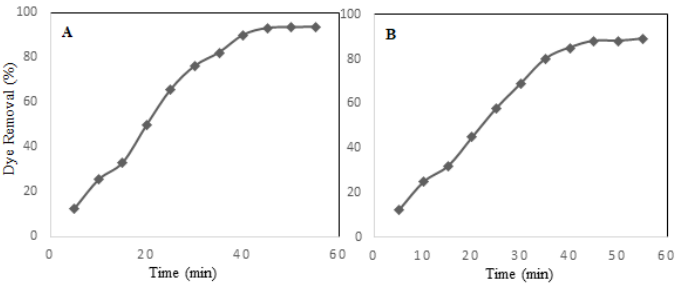

Figure 6. Effect of radiation time on removal efficiency of (A) MG and (B) MO dyes.

3.2.4. Effect of initial solution concentration.

The effect of initial dye concentration on the removal efficiency was investigated between 5 to 30 ppm for MG and 5 to 25 ppm for MO. According to Fig. 7, the photocatalytic process is more effective at a concentration of 20 ppm for MG and 15 ppm for MO.

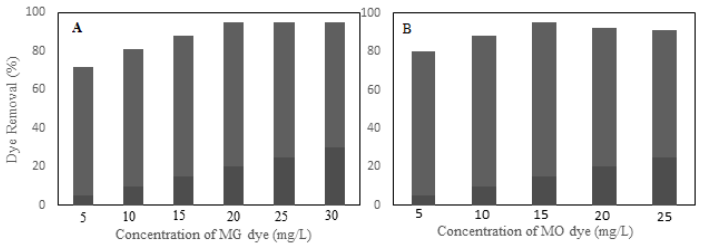

Figure 7. Effect of solution concentration on removal efficiency of (A) MG and (B) MO dyes.

3.2.5. Stability and reuse investigation.

Stability and reuse of photocatalyst in MG and MO degradation were investigated under optimum conditions. As seen in Fig. 8, the photocatalytic activity of CeO_2 nanoparticles remained without changes after four times recycle.

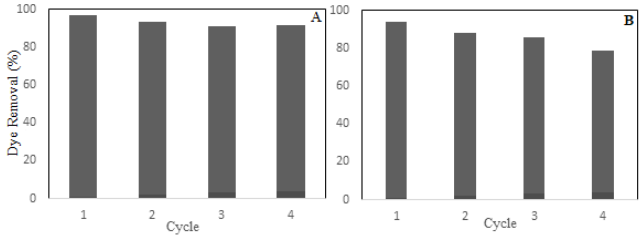

Figure 8. Investigation of photocatalyst reusability in the (A) MG and (B) MO removal.

3.2.6. Investigation of photocatalytic degradation kinetics.

Equation (1) is first-pseudo kinetic model equation in which q_e is the amount of removed dye in balancing (mg g^{-1}), q_t is the deleted dye amount at t time (mg g^{-1}) and K_1 is the first -pseudo order speed constant (min^{-1}).

$$\text{Equation (1)}: \quad \log(q_e - q_t) = \log q_e - \frac{K_1 t}{2.303}$$

Equation (2) is second -pseudo kinetic model equation in which k_2 is the second-pseudo order speed constant (min^{-1}).

$$\text{Equation (2)}: \frac{1}{q_e^2 K_2} + \frac{t}{q_e} = \frac{t}{q_t}$$

According to Fig. 9 the parameters of first-pseudo and second -pseudo kinetic was calculated (Table 3,4). As shown, the degradation of MG and MO in the presence of proposed photocatalyst is based on First -pseudo-model.

Table 3. Parameters for the removal of MG.

q_e(exp)	First pseudo-model			Second pseudo-model		
2.002	K_1 (min^{-1})	q_{e1} ($mg.g^{-1}$)	R^2	K_2 (min^{-1})	q_{e2} ($mg.g^{-1}$)	$\mathbf{R^2}$
	0.3194	1.91	0.9924	1.4359	0.4352	**0.7187**

Table 4. Parameters for the removal of MO.

q_e(exp)	First pseudo-model			Second pseudo-model		
1.8736	K_1 (min^{-1})	q_{e1} ($mg.g^{-1}$)	R^2	K_2 (min^{-1})	q_{e2} ($mg.g^{-1}$)	$\mathbf{R^2}$
	0.2726	1.780	0.9953	1.6129	0.4072	**0.9095**

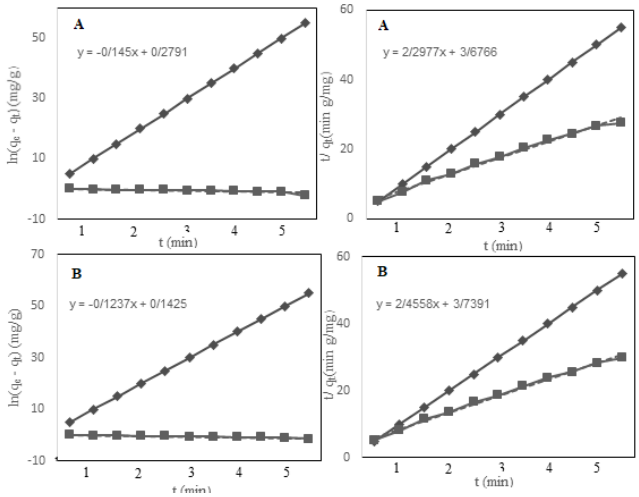

Figure 9. Kinetic model of First-pseudo and Second -pseudo for (A) MG and (B) MO removal.

3.2.7. Comparison of proposed photocatalyst with other photocatalysts.

In Table (5,6), the proposed photocatalyst was compared with other photocatalysts published in papers to remove MG and MO. CeO_2 nanostructure can remove more MG and MO with less photocatalyst consumption in shorter time under visible light in comparison with other photocatalysts.

Table 5. Comparison with other photocatalysts for the MG removal.

Photocatalyst	Concentration (ppm)	Photocatalyst Amount (g)	Time (min)	Ref
N-ZnO/C-dots nanocomposite	20	0.05	160	**[21]**
Platinum/zinc oxide nanoparticles	50	0.25	40	**[22]**
PC 50	20	0.05	160	**[21]**
Cadmium sulfide nanoparticles	10	0.25	60	**[23]**
Cerium oxide nanoparticles	20	0.02	45	**Present work**

Table 6. Comparison with other photocatalysts for the MO removal.

Photocatalyst	Concentration (ppm)	Photocatalyst Amount (g)	Time (min)	Ref
CeO_2 nanoparticles	50	0.03	120	**[24]**
Carbon foam-loaded nano-TiO_2	10	0.1	300	**[25]**
Nitrogen-doped TiO_2	30	0.25	180	**[26]**
ZnO:Eu nanoparticles	10	1.0	150	**[27]**
Cerium oxide nanoparticles	15	0.005	45	**Present work**

4. CONCLUSIONS

In this work, for the first time, cerium (IV) oxide nanopowders were synthesized in the presence of chicken egg white as stabilizer agent. We developed a simple and green method for preparation of nanoparticles at ambient temperature (25◦C) using CEW. The size of the nanopowders are <9 nm. The FESEM and XRD results show the particles were poly dispersed and spherical in shape. The prepared photocatalyst in this research work has an appropriate option for removing pollutants in the environment and

destroying organic materials in water due to its high photocatalytic properties, chemical stability, non-toxicity and high activity under visible light radiation. Also, effective parameters on degradation process such as dye solution, pH, photocatalyst amount and process time were optimized**.** The CeO_2 photocatalyst can be recycled easily.

5. REFERENCES

1. Chandrakala, H.N.; Ramaraj, B. Optical properties and structural characteristics of zinc oxide-cerium oxide doped polyvinyl alcohol films. *J. Alloys Compd* **2014**, *586*, 333-342. https://doi.org/10.1016/j.jallcom.2013.09.194.
2. Ma, R.; Zhang, S.; Wen, T.; Gu, P.; Li, L.; Zhao, G.; Niu, F.; Huang, Q.; Tang, Z.; Wang, X. A critical review on visible-light-response CeO2-based photocatalysts with enhanced photooxidation of organic pollutants. *Catal. Today* **2019**, 335, 20-30. https://doi.org/10.1016/j.cattod.2018.11.016
3. Lee, B.; Nakayama, T.; Tokoi, Y.; Suzuki, T.; Niihara, K. Synthesis of CeO2/TiO2 NPs by laser ablation of Ti target in cerium (III) nitrate hexahydrate (Ce(NO3).6H2O) aqueous solution. *J. Alloys Compd.* **2011**, *509*, 1231-1235, https://doi.org/10.1016/j.jallcom.2010.09.197.
4. Gangopadhyay, S.; Frolov, D.D.; Masunov, A.E.; Seal, S. Structure and properties of cerium oxides in bulk and nanoparticulate forms. *J. Alloys Compd* **2014**, *584*, 199-208, https://doi.org/10.1016/j.jallcom.2013.09.013.
5. Zhao, W.; Wei, Z.; Zhang, X.; Ding, M.; Huang, S.; Yang, S. Magnetic recyclable MnFe2O4/CeO2/SnS2 ternary nano-photocatalyst for photo-Fenton degradation. *Appl. Catal. A: Gen.* **2020**, 593, 117443. https://doi.org/10.1016/j.apcata.2020.117443
6. Dai, J.; Guo, Y.; Xu, L.; Zhuang, G.; Zheng, Y.; Sun, D.; Huang, J.;. Li, Q. Bovine serum albumin templated porous CeO2 to support Au catalyst for benzene oxidation. *Mol. Catal.* **2020**, 486, 110849. https://doi.org/10.1016/j.mcat.2020.110849
7. Zhao, H.; Yin, S.; Chen, Q.; Huang, X.; Chen, H.; Lu, L.; Zheng, C.; Gao, X.; Wu, T. CeO2 based catalysts for elemental mercury capture. *Energy Procedia* **2019**, 158, 4635-4640. https://doi.org/10.1016/j.egypro.2019.01.743
8. Liu, W.; Zhou, J.; Hu, Z. Nano-sized g-C3N4 thin layer @ CeO2 sphere core-shell photocatalyst combined with H2O2 to degrade doxycycline in water under visible light irradiation. *Sep. Purif. Technol.* **2019**, 227, 115665.
9. Ketzial, J.J.; Nesaraj, A.S. Synthesis of CeO2 NPs by chemical precipitation and the effects of a surfactant on the distribution of particles sizes. *J. Ceram. Process. Res*. **2011**, *12*, 74-79.
10. Arumugam, A., Karthikeyan, C., Hameed, A.S.H., Gopinath, K., Gowri, S., Karthika, V., 2015. Synthesis of cerium oxide NPs using Gloriosa superba L. leaf extract and their structural, optical and antibacterial properties. *Mater. Sci. Eng. C* **2014**, 49, 408-415, https://doi.org/10.1016/j.msec.2015.01.042.
11. Alfuraydi, A.A.; Devanesan, S.; Al-Ansari, M.; AlSalhi, M.S.; Ranjitsingh, A.J. Eco-friendly green synthesis of silver nanoparticles from the sesame oil cake and its potential anticancer and antimicrobial activities. *J. Photochem. Photobiol. B* **2019**, 192, 83-89. https://doi.org/10.1016/j.jphotobiol.2019.01.011
12. Chen, Q.; Li, X.; Xie, R.; Xu, L.; Liu, L. Novel rapid synthesis of nanoscale tungsten nitride using non-toxic nitrogen source. *Ceram. Int*. **2020**. 46, 2580-2584. https://doi.org/10.1016/j.ceramint.2019.09.221
13. Mohapatra, B.; Kuriakose, S.; Mohapatra, S. Rapid green synthesis of silver NPs and nanorods using Piper nigrum extract. *J. Alloys Compd* **2015**, *637*, 119-126, https://doi.org/10.1016/j.jallcom.2015.02.206.
14 Nethravathi, P.C.; Shruthi, G.S.; Suresh, D.; Nagabhushana, H.; Sharma, S.C. Garcinia xanthochymus mediated green synthesis of ZnO NPs: photoluminescence, photocatalytic and antioxidant activity studies. *Ceram. Int.* **2015**, *41*, 8680-8687, https://doi.org/10.1016/j.ceramint.2015.03.084.
15. Sharma, J.K.; Akhtar, M.; Ameen, S.; Srivastava, P.; Singh, G. Green synthesis of CuO NPs with leaf extract of Calotropis gigantea and its dye-sensitized solar cells applications. *J. Alloys Compd.* **2015**, *632*, 321-325, https://doi.org/10.1016/j.jallcom.2015.01.172.
16. Bala, N.; Saha, S.; Chakraborty, M.; Maiti, M.; Das, S.; Basu, R.; Nandy, P. Green synthesis of zinc oxide NPs using Hibiscus subdariffa leaf extract: effect of temperature on synthesis, anti-bacterial activity and anti-diabetic activity. *RSC Adv*. **2014**, *7*, 4993-5003, https://doi.org/10.1039/C4RA12784F.
17. Panda, K.K.; M. Achary, V.M.; Phaomie, G.; Sahu, H.K., Parinandi, N.L.; Panda, B.B. Polyvinyl polypyrrolidone attenuates genotoxicity of silver nanoparticles synthesized via green route, tested in Lathyrus sativus L. root bioassay. *Mut. Res/Gen. Toxic. Environ. Mutag.* **2016**, 806, 11-23. https://doi.org/10.1016/j.mrgentox.2016.05.006
18. Josepha, D.; Geckelera, K.E. Synthesis of highly fluorescent gold nanoclusters using egg whiteproteins, *J. Colloids Surf B: Biointerfaces* **2014**, *115*, 46-50, https://doi.org/10.1016/j.colsurfb.2013.11.017.
19. Gabal, M.A.; El-Shishtawy, R.M.; AlAngari, Y.M. Structural and magnetic properties of nano-crystalline Ni–Zn ferrites synthesized using egg-white precursor. *J. Magn. Magn. Mater.* **2012**, *324*, 2258-2264, https://doi.org/10.1016/j.jmmm.2012.02.112.
20. Duttaa, D.; Mukherjeea, R.; Patraa, M.; Banika, M.; Dasguptaa, R.; Mukherjeeb, M.; Green synthesized cerium oxide nanoparticle: A prospective drugagainst oxidative harm Basu. *J. Colloids Surf B: Biointerfaces* **2016**, *147*, 45-53, https://doi.org/10.1016/j.colsurfb.2016.07.045.
21. Sharma, S.; Mehta, S.K.; Kansal, S.K. N doped ZnO/C-dots nanoflowers as visible light driven photocatalyst for the degradation of malachite green dye in aqueous phase. *J. Alloys Compd.* **2017**, *699*, 323-333, https://doi.org/10.1016/j.jallcom.2016.12.408.
22. Reda, M.; McKinney, D.; Kadi, M.; Mkhalid, I.; Sigmun, W. Platinum/zinc oxide nanoparticles: Enhanced photocatalysts degrade malachite green dye under visible light conditions. *Ceram. Int.* **2016**, *42*, 9375-9381, https://doi.org/10.1016/j.ceramint.2016.02.147.
23. Kaur, M.; Mehta, S.; Kumar, S. Visible light driven photocatalytic degradation of ofloxacin and malachite green dye using cadmium sulphide nanoparticles. *J. Environ. Chem. Eng.* **2018**, *6*, 3631-3639, https://doi.org/10.1016/j.jece.2017.04.006.
24. Balavi, H.; Samadanian-Isfahani, S.; Mehrabani-Zeinabad, M.; Edrissi, M. Preparation and optimization of CeO2 nanoparticles and its application in photocatalytic degradation of Reactive Orange 16 dye. *Powder Technol*. **2013**, *249*, 549-555, https://doi.org/10.1016/j.powtec.2013.09.021.
25. Chuang, W.; Zhen-Hai, S.; Lei, P.; Wen-min, H.; Bingliang, L.; Kezhi, L. Preparation of carbon foam-loaded nano-TiO_2 photocatalyst and its degradation on methyl orange. *Surf. Interfaces*. **2017**, *7*, 116-124, https://doi.org/10.1016/j.surfin.2017.03.007.
26. Nasirian, M.; Mehrvar, M. Photocatalytic degradation of aqueous Methyl Orange using nitrogen-doped TiO_2 photocatalyst prepared by novel method of ultraviolet-assisted thermal

synthesis. *J. Environ. Sci.* **2018**, *66*, 81-93, https://doi.org/10.1016/j.jes.2017.05.032.
27. Trandafilovic, L.V.; Jovanovic, D.J.; Zhang, X.; Ptasinska, S.; Dramicanin, M.D. Enhanced photocatalytic degradation of methylene blue and methyl orange by ZnO:Eu nanoparticles, *Appl. Catal. B: Environ.* **2016**, *203*, 740-752, https://doi.org/10.1016/j.apcatb.2016.10.063.

6. ACKNOWLEDGMENT

The authors would like to express their sincere appreciation to the founders of the Shahid Bahonar University of Kerman, Mr. Alireza Afzalipour and his wife, Mrs. Fakhereh Saba, for their foresight and generosity in training future generations of doctors, engineers and scientists. Also, the authors would like to acknowledge their thanks to Dr. Parviz Dabiri for his generous support for the research activities of the chemistry and nano laboratories in the Shahid Bahonar University of Kerman.